UACEE International Journal of Advancements in Electronics and Electrical Engineering – IJAEEE
Volume 2 : Issue 2 [ISSN 2319 – 7498]
Publication Date : 05 June 2013

Robust Load Frequency Control of Two-Area Power System along with Coordinated Operation of TCPS-SMES

[a]S. K. Pandey, [b]S R Mohanty, *Member, IEEE* , [b]Nand Kishor *Member, IEEE,* [c]P K Ray

[a]Research scholar in Department of Electrical Engineering, Motilal Nehru national Institute of Technology Allahabad, India
[b]Department of Electrical Engineering, Motilal Nehru national Institute of Technology Allahabad, India
[c]Department of Electrical and Electronics Engineering, IIIT, Bhubaneswar, India
(e-mail: skp1111.1969@rediffmail.com; soumyaigit@gmail.com; pkrayiiit@gmail.com)

Abstract. This paper presented a design of a decentralized robust proportional-integral-derivative controller based on Linear Matrix Inequality (LMI) approach for two-area interconnected power system with multi-unit comprising of non-reheat and reheat steam turbine in each control area along with coordinated operation of Thyristor Controlled Phase Shifter (TCPS) and Superconducting Magnetic Energy Storage (SMES) for load frequency control (LFC). In this work PID control problem is reduced to a static output feedback control synthesis through H_∞ control approach, and then design two controllers one is H_∞ controller and second is iterative proportional-integral-derivative (IPIDH$_\infty$) controller based on LMI approach. The simulation results show that the IPIDH$_\infty$ is superior to robust H_∞ controller. The robustness of both controllers is also tested with different load scenarios and also with parameters variations.

Keywords: Robust control, TCPS, linear matrix inequalities, PID controller, SMES, H_∞ control.

1. Introduction

One of the important aspects of automatic generation control (AGC) of power system is to maintain of frequency and power change over the tie-lines at their specified values. This is achieved by LFC. In case of conventional control strategy for the LFC problem the integral of the area control error (ACE) is taken as the control signal. An integral controller gives zero steady state deviation, but it exhibits poor dynamic behavior. In the past decades, the LFC problem tackled by conventional proportional integral (PI) controller. The LFC using genetic algorithms and linear matrix inequalities is proposed in [1], while ILMI algorithm based LFC is given in [2], and AGC with fuzzy logic controller for the power system including SMES units is discussed in [3]. The AGC of hydro-thermal power system with SMES is presented in [4]. The design of decentralized controller for LFC using genetic algorithm of interconnected two-area power systems with RFB considering TCPS in the tie-line is given in [5]. Load frequency stabilization by coordinated control of TCPS and SMES for three types of interconnected two-area power systems is discussed in [6]. Fuzzy logic based LFC of two-area power systems with SMES is given in [7]-[8].

In this paper, the LFC problem is formulated as a H_∞-static output feedback (SOF) control problem to obtain a desired PID controller based on an iterative linear matrix inequality (ILMI) [9]. The optimization problem has been formulated and control parameters of IPIDH$_\infty$ controller is carried out through ILMI algorithm. It is easy to implement in real systems. The robustness of the proposed controller has been evaluated in two-area interconnected power systems along with coordinated operation of TCPS-SMES with different scenarios. Simulation results show that the robustness of the IPIDH$_\infty$ controller is much superior to that of the H_∞ controller against various load changes and parameters variations.

2. INTEGRATION OF SMES AND TCPS WITH TWO-AREA POWER SYSTEM

The proposed two-area interconnected power system with TCPS in series with tie-line and SMES units connected in each area is as shown in Fig. 1. As the recent in power electronics have led to the development of the FACT devices. Which are designed to overcome the limitations of the mechanically controlled devices used in the power systems and enhance power system stability using reliable and high-speed electronic components. The detailed about SMES unit is mentioned in [3].

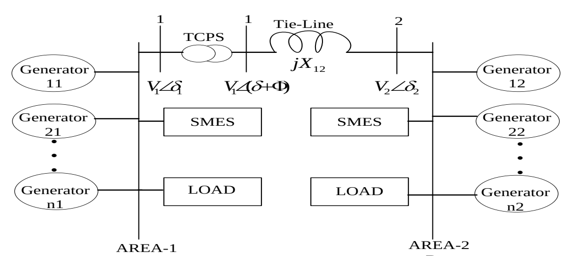

Fig. 1. Schematic of a two-area power system with TCPS in series with tie-line and SMES units connected in each area.

2.1 Tie-line Power Flow Model Considering TCPS and its Control Strategy

In this study, a two-area thermal power system interconnected by a tie-line through with series connection of TCPS is considered as shown in Fig. 1. TCPS is placed near Area 1. The incremental tie-line power flow from area 1 to area 2, without TCPS can be expressed as [5]

$$\Delta P_{tie12}^{0} = \frac{2\pi T_{12}^{0}}{s}(\Delta f_1 - \Delta f_2) \tag{1}$$

While, the incremental tie-line power flow from area 1 to area 2, with TCPS can be expressed as [5]

$$\Delta P_{tie12}(s) = \frac{2\pi T_{12}}{s}[\Delta F_1(s) - \Delta F_2(s)] + T_{12}\frac{K_\phi}{1+sT_{ps}}\Delta Error_1(s) \tag{2}$$

In case of TCPS control strategy, $\Delta Error_1$ can be any signal such as the area frequency deviation or the ACE to the TCPS unit to control the TCPS phase shifter angle which in turn controls the tie-line power flow. But in this study case TCPS is placed near to area 1, therefore, consider, the control signal to the TCPS unit is Δf_1, because the measurement of Δf_1 will be easier rather than ACE_1.
Therefore, equation (2) becomes as

$$\Delta P_{tie12}(s) = \frac{2\pi T_{12}}{s}[\Delta F_1(s) - \Delta F_2(s)] + T_{12}\frac{K_\phi}{1+sT_{ps}}\Delta f_1 \tag{3}$$

The detailed of tie-line power flow model with TCPS is discussed in [5].

2.2 Superconducting Magnetic Energy Storage (SMES) Devices [3]

When power demand is suddenly increases in a control area, the stored energy is almost immediately released by the SMES through its power conversion system (PCS). As the governor control mechanism starts working to set the power to the new equilibrium condition, the SMES coil stores energy back to its nominal level. Similar action happens when there is a sudden decrease in load demand. In LFC operation, the dc voltage across the superconducting inductor is continuously controlled depending on the sensed ACE signal.
In this study, inductor voltage deviation ΔE_d of SMES unit of each area is based on ACE of the same area in power system. Fig. 2 shows the block diagram of SMES unit [3].

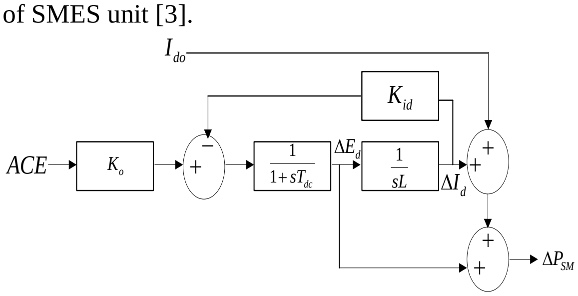

Fig. 2. Block diagram of SMES control scheme [3].

3. CONTROL APROACH

This section gives a brief overview of robust H_∞ control and robust iterative PIDH$_\infty$ control design via LMI approach.

3.1 Design of H_∞ Controller via LMI Approach

The objective of H_∞ control theory is to design the control law u on the basis of the measured variable y, so that the effect of the disturbance ω on the control variable z_∞, expressed in terms of the infinity norm of the transfer function from z_∞ to w i.e. $\|T_{z\infty w}\|$ does not exceed a specified limit γ defined as guaranteed robust performance. The classical closed-loop system via robust H_∞ control [1] is represented as shown in Fig. 3. The state space representation of system *P(s)* model is given by [1]:

$$\begin{aligned} \dot{x} &= Ax + B_1 w + B_2 u \\ z_\infty &= C_1 x + D_{11} w + D_{12} u \\ y &= C_2 x + D_{21} w + D_{22} u \end{aligned} \tag{4}$$

Where, x is a state variable. The state space of controller $K_\infty(s)$ model is assumed as follows [1]:

$$\begin{aligned} \dot{\xi} &= A_k \xi + B_k y \\ u &= C_k \xi + D_k y \end{aligned} \tag{5}$$

Where ξ is the state variable for controller model.

Combining equations (4) and (5), provided that (A, B_2) is stabilizable and (A, C_2) is detectable, the following closed-space model will be achieved:

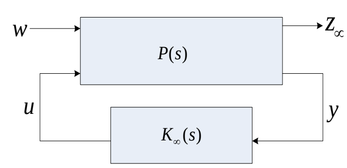

Fig. 3. Close-loop system via H_∞ control.

$$\begin{aligned} \dot{x}_{cl} &= A_{cl} x_{cl} + B_{cl} w \\ z_\infty &= C_{cl} x_{cl} + D_{cl} w \end{aligned} \tag{6}$$

The closed-loop root mean square (RMS) gain $T_\infty(s)$ or H_∞ norm of the transfer function $\|T_{z_\infty w}\|$, does not exceed performance index γ, if and only if there exists a symmetric matrix X_∞ [1] such that

$$\begin{bmatrix} A_{cl}X_\infty + X_\infty A_{cl}^T & B_{cl} & X_\infty C_{cl}^T \\ B_{cl}^T & -I & D_{cl}^T \\ C_{cl}X_\infty & D_{cl} & -\gamma^2 I \end{bmatrix} < 0 \tag{7}$$

$$X_\infty > 0 \tag{8}$$

Hence, the optimal H_∞ control is achieved by minimizing the performance index γ, subject to the matrix inequalities (7) and (8).

3.2 Design of Iterative PIDH-infinity (IPIDH$_\infty$) Controller via LMI Approach

Consider the system model is defined as

$$\dot{x} = Ax + B_1 w + B_2 u$$
$$z_\infty = C_1 x + D_{12} u \qquad (9)$$
$$y = C_2 x$$

The PID controller defined as:

$$u = K_1 y + K_2 \int_0^t y dt + K_3 \frac{dy}{dt} \qquad (10)$$

Where, K_1, K_2 and K_3 matrices to be designed (PID gains). The output feedback H_∞-control problem is to find a controller of the form

$$u = Ky \qquad (11)$$

such that the infinite-norm of the closed-loop transfer function from z_∞ to w

$$\left\| T_{z_\infty w} \right\|_\infty < \gamma \qquad (12)$$

Let $z_1 = x$, $z_2 = \int_0^t y dt$, and $z = \begin{bmatrix} z_1 \\ z_2 \end{bmatrix}$, the new state variables then the problem of a PID is reduced to a static output feedback (SOF) control system as

$$\dot{z} = \bar{A} z + \bar{B}_1 w + \bar{B}_2 u$$
$$\bar{z}_\infty = \bar{C}_1 z + \bar{D}_{12} u \qquad (13)$$
$$\bar{y} = \bar{C}_2 z + \bar{D}_{21} w$$
$$u = \bar{K} \bar{y}$$

Where, $\bar{A} = \begin{bmatrix} A & 0 \\ C_2 & 0 \end{bmatrix}$, $\bar{B}_1 = \begin{bmatrix} B_1 \\ 0 \end{bmatrix}$, $\bar{B}_2 = \begin{bmatrix} B_2 \\ 0 \end{bmatrix}$,

$$\bar{C}_1 = \begin{bmatrix} C_1 & 0 \end{bmatrix}, \; \bar{C}_2 = \begin{bmatrix} \bar{C}_{21} & \bar{C}_{22} & \bar{C}_{23} \end{bmatrix}^T$$
$$\bar{D}_{12} = D_{12}, \; \bar{D}_{21} = \begin{bmatrix} 0 & 0 & C_2 B_1 \end{bmatrix}^T \qquad (14)$$
$$\text{and } \bar{K} = \begin{bmatrix} \bar{K}_1 & \bar{K}_2 & \bar{K}_3 \end{bmatrix} \qquad (15)$$

Once $\bar{K}$ is found, the original PID gains can be obtained from

$$K_3 = \bar{K}_3 \left(I + C_2 B_2 \bar{K}_3 \right)^{-1}, K_2 = \left(I - K_3 C_2 B_2 \right) \bar{K}_2,$$
$$K_1 = \left(I - K_3 C_2 B_2 \right) \bar{K}_1 \qquad (16)$$

The algorithm of an iterative *PIDH$_\infty$* via LMI approach for the optimization problem mentioned in equation (12) is as follows [9]:

Step 1: Form the state space model of the system (A, B_1, B_2, C_1, C_2, and D_{12}), then compute $\bar{A}$, $\bar{B}_1$, $\bar{B}_2$, $\bar{C}_1$, and $\bar{C}_2$ as defined in equation (13) and select the performance index γ.

Step 2: Select $Q > 0$ and solve P for the Riccati equation $\bar{A}^T P + P\bar{A} - P\bar{B}_2 \bar{B}_2^T P + Q = 0$, $P > 0$ Set $i = 1$ and $X_i = P$.

Step 3: Solve the following optimization problem for P_i, $\bar{K}$ and a_i.

Optimization 1: Minimize a_i subject to the following LMI constraints [9]

$$\begin{bmatrix} \Sigma & P_i \bar{B}_1 & (\bar{C}_1 + \bar{D}_{12} \bar{K} \bar{C}_2)^T & (\bar{B}_2^T P_i + \bar{K} \bar{C}_2)^T \\ \bar{B}_1^T P_i & -\gamma & 0 & 0 \\ \bar{C}_1 + \bar{D}_{12} \bar{K} \bar{C}_2 & 0 & -I & 0 \\ \bar{B}_2^T P_i + \bar{K} \bar{C}_2 & 0 & 0 & -I \end{bmatrix} < 0 \qquad (17)$$

Where, $\Sigma = \bar{A}^T P_i + P_i \bar{A} - X_i \bar{B}_2 \bar{B}_2^T P_i - P_i \bar{B}_2 \bar{B}_2^T X_i + X_i \bar{B}_2 \bar{B}_2^T X_i - a_i P_i$

Denote by a_i^* the minimized value of a_i.

Step 4: If $a_i^* \le 0$, the matrix pair $(P_i, \bar{K})$ solves the problem. Stop. Otherwise go to Step 5.

Step 5: Solve the following optimization problem for P_i and $\bar{K}$.

Optimization 2: Minimize trace(P_i) subject to LMI constraints (17) with $a_i = a_i^*$. Denote by P_i^* the optimal P_i.

Step 6: If $\left\| X_i \bar{B}_1 - P_i^* \bar{B}_1 \right\| < \varepsilon$, Where ε is a prescribed tolerance, go to Step 7; otherwise set $i = i + 1$, $X_i = P_i^*$, and go to Step 3.

Step 7: If obtained solution $\bar{K}$ satisfies the gain constant, it is desirable, otherwise change constant weights (n_i), Q and γ and go to step 1.

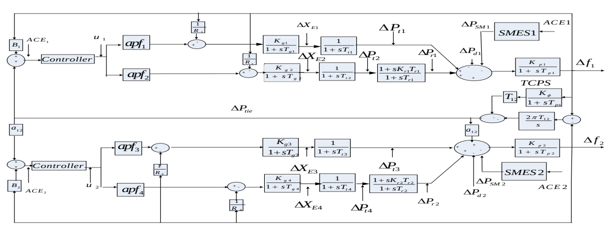

Fig. 4. Two areas reheat thermal power system model.

4. SIMULATION RESULTS

This section discusses the simulation analysis by above described controllers for two-area power system along with coordination of TCPS and SMES as shown in Fig. 4. The response is tested for the different load conditions. The same parameters of power system with TCPS and [6]-[7] for SMES for the system under study have been taken.

4.1 Step load change

In this case, the increasing load disturbances of $\Delta P_{d1} = 0.01 pu$ and $\Delta P_{d2} = 0.01 pu$ applied to the system. The frequency deviation Δf_1, Δf_2 and change in tie-power line ΔP_{tie} are shown in Fig. 5. The peak frequency deviation is very small and reduced significantly to zero within shorter period in case of IPIDH$_\infty$ controller.

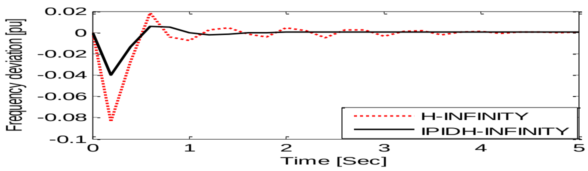

(a) Frequency deviation in area 1

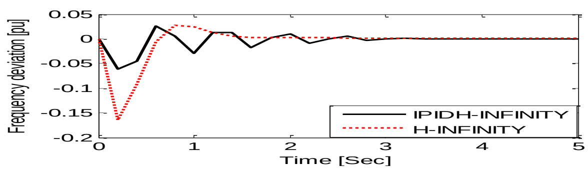

(b) Frequency deviation in area 2.

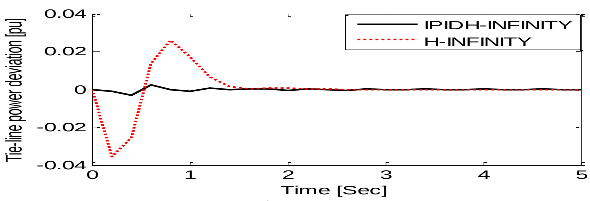

(c) Tie-line power deviation of power system.

Fig. 5 Responses of power system with increasing step loads.

4.2 Random step load change in area 1

In this case consider the load disturbance ΔP_{d1} being varied in steps as shown in Fig. 6, with $\Delta P_{d2} = 0.01 pu$ applied to the system. The purpose of this scenario is to test the robustness of the proposed controller against varying disturbances. The corresponding responses of the power system are shown in Fig. 7. It is observed that IPIDH$_\infty$ controller achieves comparatively better damping for frequency deviation profile.

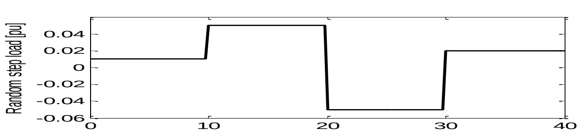

Fig. 6. Random load change in step form.

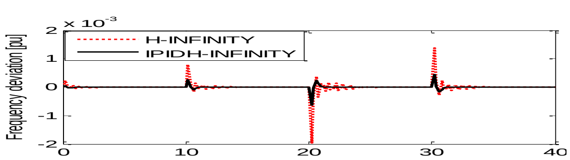

(a) Frequency deviation in area 1.

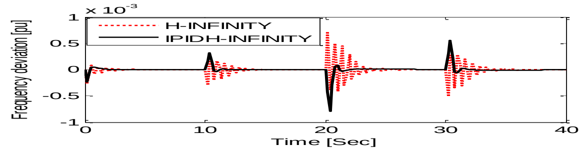

(b) Frequency deviation in area 2.

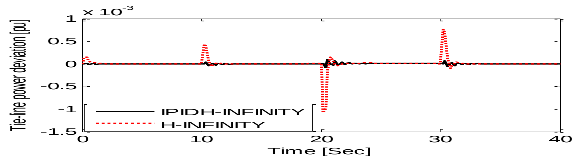

(c) Tie-line power deviation of power system.

Fig. 7. Responses of power system with step load variation.

4.3 Random load change in area 1

In this case, the random load change as shown in Fig. 8 for ΔP_{d1} and $\Delta P_{d2} = 0.01 pu$ applied to the system. The responses of power system are shown in Fig. 9. The control effect of the proposed IPIDH$_\infty$ controller is superior to that of the H$_\infty$ controller. The response is characterized by low overshoot/undershoot, less oscillation and faster response.

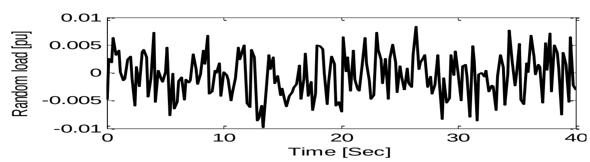

Fig. 8 Random load change.

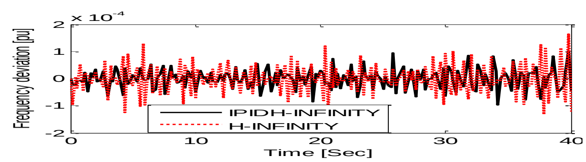

(a) Frequency deviation in area 1.

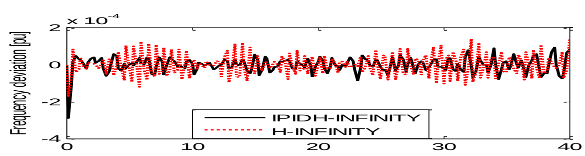

(b)Frequency deviation in area 2.

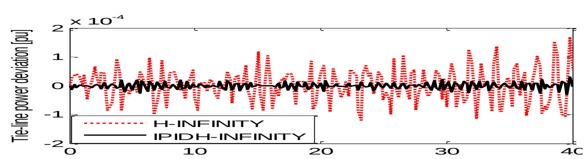

(c) Tie-line power deviation of power system.

Fig. 9. Responses of power system with random load change in area 1.

UACEE International Journal of Advancements in Electronics and Electrical Engineering – IJAEEE
Volume 2 : Issue 2 [ISSN 2319 – 7498]
Publication Date : 05 June 2013

4.4 Robustness with parameter variations

The robustness of the proposed two controllers is evaluated by computation of integral square error (ISE) under variation in system parameters. In order to be realistic, the simulations were done for a limited time. Moreover, the integral values are multiplied by some suitable constants so that the outcomes of the performance indices attain comparable values. Therefore, the ISE performance index modified as:

$$\Delta f_{ISE} = 10^4 \int_0^{40} (\Delta f_1^2 + \Delta f_2^2 + \Delta P_{tie}^2) dt$$

The values of ISE against parameters changes for the H∞ and IPIDH∞ controllers are shown in Fig. 10. As observed with change in parameters over a large percentage range, the corresponding values of ISE gets varied significantly increase in case of H∞ controller. On the other hand, the values of ISE with IPIDH∞ controller are much lower and change slightly. These simulation results confirm the high robustness of IPIDH∞ controller against the load change, and system parameter variations.

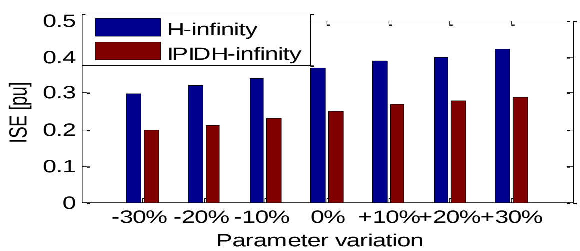

Fig. 10 Evaluation of robustness by computing ISE for all parameters variation.

Nomenclature

Δf_i Deviation in frequency, K_{gi} Gain of governor system, T_{gi} Time constant of the governing mechanism in seconds, K_{ti} Gain of turbine system, T_{ti} Time constant of the turbine in seconds, K_{ri} Gain of reheat steam turbine system, K_{pi} Subsystem equivalent gain, T_{ri} Time constant of the reheat steam turbine in seconds, B_i Frequency bias, T_{pi} Time constant of the subsystem equivalent in seconds, T_{12} Tie-line synchronizing coefficient between area 1 and 2, ΔP_{di} Load deviation, R_i Droop characteristic, P_{tie} Tie-line power flow, ACE_i Area control error, ΔX_{Ei} Governor Valve position, ΔP_{ti} Turbine power, ΔP_{ri} Reheat steam turbine power, apf_i Area participation factor, $\Delta \phi$ Phase shifter angle.

5. CONCLUSIONS

This paper presented a decentralized robust iterative PID controller based LMI approach for two-area interconnected power system with multi-unit comprising of non-reheat and reheat steam turbine in each control area along with coordinated operation of TCPS and SMES for load frequency control (LFC) problem. In this work PID control problem is reduced to a static output feedback control synthesis through H∞ control approach, and then design two controllers one is H∞ controller and second is ILMI algorithm based iterative proportional-integral-derivative (IPIDH∞) controller. The optimization problem was formulated and iterative PIDH∞ algorithm is used to tune the control parameters. Thus the simulation results reflect IPIDH∞ is superior to robust H∞ control in its performance subjected to parameter variation as well as uncertainty in the load variation.

References

1. Rerkpreedapong, D., Hasanovic, A., and Feliachi, A., “Robust load frequency control using genetic algorithms and linear matrix inequalities,” IEEE Trans. on Power Syst. 18(2), pp. 855-861, (2003).
2. Bewrani, H., Mitani, Y., and Tsuji, K., “Robust decentralized load frequency control using an iterative linear matrix inequalities algorithm,” IEE Proc. Gener. Trans. Distrib. 151(3), pp. 347-354, (2004).
3. Demiroren, D., and Yesil, E., “Automatic generation control with fuzzy logic controllers in the power system including SMES units,” Electric Power and Energy Systems. 26, pp. 291-305, (2004).
4. Abraham, R. J., Das, D., and Patra, A., “Automatic generation control of an interconnected hydrothermal power system considering Superconducting Magnetic Energy Storage,” Electrical Power and Energy Systems. 29, pp. 271-579, (2007).
5. Chidambaram, I. A., and Paramasivam, B., “Genetic algorithm based decentralized controller for load-frequency control of interconnected power systems with RFB considering TCPS in the tie-line,” Intr. Journal of Electronic Engineering Research. 1(4), pp. 299-312, (2009).
6. P.Bhatt, S.P.Ghoshal, and R.Roy, “Load frequency stabilization by coordinated control of Thyristor Controlled Phase Shifters and superconducting magnetic energy storage for three types of interconnected two-area power systems,” Electric Power and Energy Systems. 32, pp.1111 -1124, (2010).
7. A.M.Hemeida, “A fuzzy logic controlled superconducting magnetic energy storage, SMES frequency stabilizer,” Electric Power and Energy Systems. 80, pp. 651-656, (2010).
8. K.R.Sudha, and R.V.Santhi, “Load frequency control of an interconnected reheat thermal system using type-2 fuzzy systems including SMES units,” Electric Power and Energy Systems. 43, pp. 1383-1392, (2012).
9. Ahmed Bensenouci, “Robust iterative PID controller based on linear matrix inequality for a sample power system” World Academy of Science, Engineering and Technology 21 2008, pp. 611-619.